Z. Phys. Chem. **225** (2011) 183–216 / **DOI** 10.1524/zpch.2011.0054

Inelastic Neutron Scattering (INS) Study of Low Frequency Vibrations and Hydrogen Bonding of (*E*)-2-Hydroxyimino-2-Cyanoacetic Acid Ethyl Ester

By M. Rachwalska[1,*], I. Natkaniec[2,3], K. Hołderna-Natkaniec[4], Z. H. Urbanek[1], and K. K. Zborowski[1]

[1] Faculty of Chemistry, Jagiellonian University, 30-060 Kraków, Poland
[2] H. Niewodniczanski Institute of Nuclear Physics, PAS, 31-342 Kraków, Poland
[3] Frank Laboratory of Neutron Physics, JINR, 141980 Dubna, Russia
[4] Faculty of Physics, A. Mickiewicz University, 61-614 Poznań, Poland

(Received September 19, 2010; accepted September 28, 2010)

(E)-Cyano-Oxime / (E)-Configuration / S-Cis,S-Trans Rotational Isomerism / Conformer (Rotamer) / Infrared (IR) / Raman Spectroscopy / IINS / Density Functional Theory (DFT)

The title unsubstituted (normal) (*E*)-2-hydroxyimino-2-cyanoacetic acid ethyl ester (the abbreviated name: (*E*)-2-cyanoethyl ester-2-oxime or 2-oxime) and its 2-deuterated analogue have been prepared and characterized using infrared, Raman and inelastic, incoherent neutron scattering (IINS) spectroscopy. Molecular structures (molecular conformations) of the compounds are proposed for the vapour state. Four molecular conformers, namely two pairs of the s-cis, s-trans rotational isomers (rotamers) from six lower energetic conformations of *E*-2-hydroxyimino-2-cyanoacetic ethyl ester, are predominating for the single molecule of the compound. They amount together to almost 100% of the conformational populations of both rotational isomers as it was theoretically calculated using DFT (B3LYP) method with 6-311G++(d,p) basis set. Additionally dimers of 2-oxime were considered using B3LYP/6-31G* method in order to improve the results obtained for single molecule. In both parent (=N−OH) and deuterated (=N−O−D) molecules of the (*E*)-2-ethylcyano ester-2-oxime respectively, extra bands corresponding primarily to hydrogen (deuterium) bond vibrations (γ–bending out of plane of hydrogen bond, σ–stretching of hydrogen bond bridge, δ–bending in plane of hydrogen bond, λ–bending of hydrogen bond bridge have been identified, namely σ (N−O−H···O) at 132.8, 212.5, 279, 358.7, 424, 448, 523.6, 872, γ (N−O−H···O) at 334, 564, 592, 745, 820, δ (N−OH···O) at 1461, 1600, 1862 cm^{-1} in the low temperature IINS spectrum, whereas the frequency at 365 cm^{-1} has been assigned as the out of plane (o.o.p.) ($\gamma_{O-D\cdots O}$) vibrational mode. Formation of the O−H···O hydrogen bridge is reflected in shifting of the bands of the stretching and bending vibrations of OH group as well as arising of the bridge vibrations in the low frequency range. Moreover, equilibrium geometries and all harmonic vibrational frequencies of the (*E*)-2-cyano ethyl ester-2-oxime molecules with potential energy distribution (PED) were also calculated by means of the above mentioned theoretical programs.

* Corresponding author. E-mail: rachwals@chemia.uj.edu.pl

1. Introduction

Among the non-covalent interactions hydrogen bond (H-bond) is the most common and important in biologically active compounds and processes. Hydrogen bonds determine the molecular packing of the molecules in crystals and interactions in liquids and gas phase [1]. The O−H···O hydrogen bond is the strongest among others and OH group which forms the most common hydrogen bonds and can react as a proton donor (O−H) as well as a proton acceptor (···O) so the hydrogen bonds are usually arranged in a complicated hydrogen bond patterns. Among organic compounds alcohols and phenols have been intensively investigated but the other families of compounds *i.e.* oximes, have not been intensively investigated till now.

Formation of the hydrogen bond changes the structures of compounds with an OH group and a consequence of this change is reflected in the vibrational spectra. The in-plane OH (δ) and out-of-plane OH (γ) deformation bands shift to higher frequencies (so called blue shift), while the stretching band OH shifts to a lower frequency range (red shift) with an increase of O−H···O hydrogen bond strength [2]. The high frequency υ[OH] band is the most convenient for studies of hydrogen bond formation and of hydrogen bond strength, because it has got a high intensity in IR spectra. Investigations of changes in the deformation vibrations of the OH group with varying hydrogen bond strength are more difficult because of their coupling with other molecular vibrations. The INS method used in this work is especially useful in investigation of the proton vibrations in low energy transfer. It is well known that cross-section for inelastic neutron scattering takes the values: 82, 5.55, 11.51, 4.23 barns for hydrogen, carbon, nitrogen and oxygen, respectively [3]. Therefore in the IINS spectra the bands assigned to proton vibration are dominant.

The crystal structure of 2-oxime [4] confirms that this compound in solid state is engaged in complicated O−H···O hydrogen bond patterns although the precise proton location has not been determined in this X-ray structure [4] and is determined in neutron powder diffraction (NPD) spectra [5]. In this paper we decided to compare the structure (conformations) and vibrational spectra of monomer and dimer to investigate the influence of O−H···O hydrogen bond formation on the vibrational spectra. Because of the OH vibrations in 2-oxime with other molecular vibrations' coupling, it can be expected that the formation of the O−H··· hydrogen bond will strongly influence the vibrational spectrum of the proton donor and proton acceptor. Additionally, formation of the hydrogen bond changes the geometry of proton donor and proton acceptor and these changes are reflected in the vibrational spectra. The method used in this study is optimization of 2-oxime monomer and dimer structure and comparison of the theoretical vibrational spectra with experimental INS spectra to find changes caused by the formation of O−H···O hydrogen bond bridges.

(*E*)-2-hydroxyimino-2-cyanoacetic acid ethyl ester (abbreviated name: (*E*)-2-cyanoethyl ester-2-oxime or 2-oxime) which is the subject of the paper, belongs to the family of bioactive organic substances. There are many publications dealing the problem. As some examples presenting the bioactive properties of some oximes we give the following [33–36]. Many of them have been investigated for many years by IINS as for example [6–9]. About physical and chemical properties of the substance we

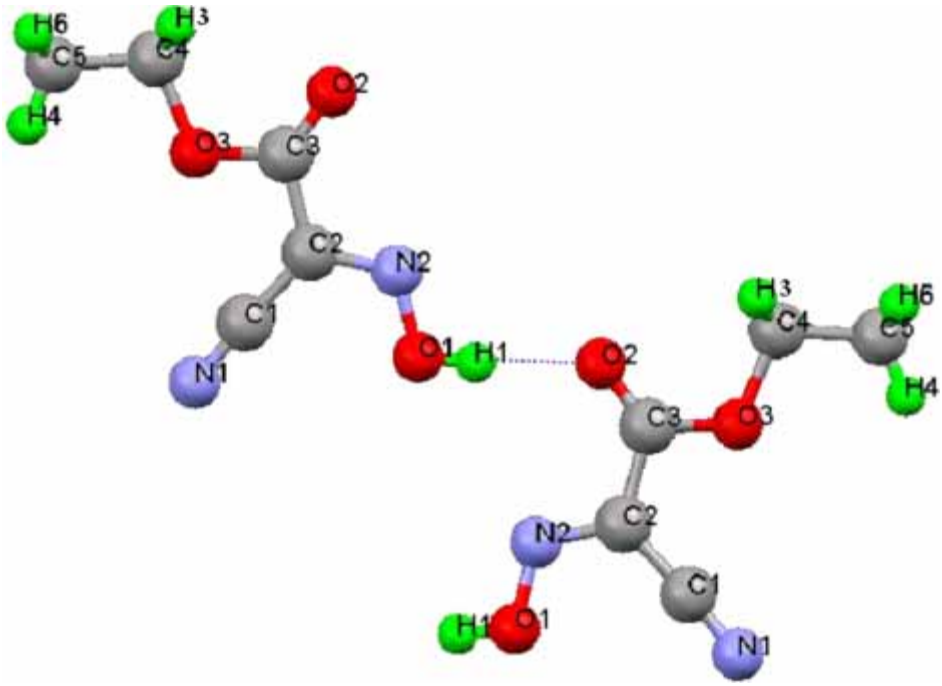

Fig. 1. (*E*)-2-hydroxyimino-2-cyanoacetic acid ethyl ester molecules in its crystal lattice showing the most "comfortable" hydrogen bond between hydrogen atom of hydroxyimino group and the oxygen atom of carbonyl group in the nearest molecule. Such the dimer has been considered in the theoretical calculations of the paper. The picture was drawn by using the crystallographic data [4].

have said in our publication [5] dealing the problem of structure of (*E*)-2-cyanoethyl ester-2-oxime, estimated at various temperatures.

This knowledge [4,5] appeared to be very important for the present theoretical calculations of the dynamics' properties of the 2-oxime molecules (see later). It is known as we said in [11] that oximes, previously investigated by Jackson [12] by using only medium IR spectroscopy, can form intermolecular hydrogen bond in the solid state in four different ways, namely:

O(1)−H1···N(2)=C(2) (I), O(1)−H1···N(1)≡C(1) (II),
O(1)−H1···O(2)=C(3) (III) and O(1)−H1···O(1)−N(2) (IV).

Numbering of all atoms of the (*E*)-2-cyanoethyl ester-2-oxime molecule is presented in Fig. 1.

As to the first mode of the formation of H-bonds (*i.e.*) O(1)−H···N(2)= C(2) (I) in the case of (*E*)-2-cyanoethyl ester-2-oxime, a reduction of the π-charge at the oxime's nitrogen atom is the effect of π conjugation between an oxime group =N(2)-O(1)-H(1) and an π electron – withdrawing substituent in the oxime moiety. Therefore Jackson [12] suggested that as a result of such a conjugation, those oximes do not form H-bonds of the O−H···N=C type. On the other hand, oximes possessing keto-substituents (oximes of medium strength) may form intramolecular H-bonds O(1)−H···O(2)=C,

but this kind of association is without any effect on the $\nu_{[C=N]}$ vibrational frequency [12]. Therefore, on the basis of those considerations, 2-oxime molecule is unlikely to form intermolecular H-bonds of the O(1)−H(1)···N(2)=C(2) type (I) but can form intermolecular H-bonds of the O(1)−H···O(1)−N(2) type (IV).

Generally speaking, the phenomenon of inter molecular hydrogen bonded association is the most characteristic feature for the oximes' family. This phenomenon is demonstrated in the case of oximes of weak acidity (pK_a 10–12.5), oximes of medium acidity (pK_a 7–10) and acidic (or very acidic) oximes of pK_a 4.5–6 [13]. We mean here simple weakly conjugated oximes, also conjugated ones with one substituent electron – withdrawing at C(2) as well as oximes possessing two conjugated electron-acceptor substituent groups at C(2) and C(3) in the molecule. On intermolecular strong H-bonding one may conclude from the IR spectrum of 2-oxime in its solid state [11].

Taking into consideration the two last ways of hydrogen bond formation as the most probable in the case of the 2-oxime molecules [12], a detailed analysis of their fundamental vibrational modes, *viz.* stretching (ν), bending in plane (δ), bending out of plane (γ) and σ (connected with displacement of oxygen atoms – stretching of the hydrogen bond bridge) deformations of the oximino-group has been done and it is the essential aim of this work. Particularly in this paper an experimental evidence of out of plane γ, σ, δ deformations (in plane) of the OH in oximino-group (which may be observed in the 50–1700 cm^{-1} range) as well as ρ – out of plane internal modes and χ – torsional out of plane modes is presented.

According to the X-ray [4] and NPD results [5] the 2-oxime molecules are linked together by hydrogen bonds between the terminal O−H groups and the oxygen atoms of carbonyl of the ester groups to form zigzag chains (Fig. 1).

Some spectroscopic studies have been performed until now [9,11,12] on various kinds of C-mono-or disubstituted oximes having (*E*) or (*Z*) molecular configuration by using optical (*i.e.* IR and Raman scattering) spectroscopy, but there is still lacking analogous work using inelastic incoherent neutron scattering (IINS) as a complementary spectroscopic technique in comparison to the optical one. The last investigations allow to describe protons' dynamic at small energy transfers especially the protons' dynamic in the hydrogen bond.

Therefore we have undertaken such the investigations for (*E*)-2-cyanoethyl ester-2-oxime. As compared with optical spectroscopic methods, incoherent neutron scattering (IINS) presents a number of advantages in studying molecular vibrations in solids:

1. no selection rules are obvious in neutron spectroscopy,
2. low-wave number vibrations are the source of more intense bands than do high-wave number ones,
3. the proton incoherent cross-section is much higher than that of other nuclei (as we have already mentioned).

Consequently, the vibrational modes in which hydrogen atoms participate give rise to IINS bands with much higher intensities than the bands due to other atoms. Therefore the replacement of the hydrogen atom by deuterium, whose incoherent scattering cross section for thermal neutrons is almost ten times smaller (equal to 7.64 barn [3], while the oscillator mass is twice as large) makes it possible to identify uniquely the modes due to hydrogen vibrations of the molecules of 2-oxime. IINS spectroscopy therefore

may provide the important information about dynamic properties of organic hydrogen bonded molecules in the energy range below 900 cm^{-1}. On the other hand, Raman scattering as well as IR spectroscopy make it possible to analyze the wave-number modes located above 50 cm^{-1}, in the region 50–4000 cm^{-1}.

Finally it should be stressed here that the low-frequency vibrations of investigated compounds in the range between 50–800 cm^{-1} are easily measurable by the method of the inelastic incoherent neutron scattering (IINS), whereas the optical spectroscopy (*e.g.* infrared and Raman scattering) may not be useful sometimes for that purpose. Such a situation may happen when some fundamental vibrations (as for example, the out of plane (o.o.p.) hydrogen-bonded $\gamma_{N-H\cdots O}$ ones in the case of certain amino-acids) are inactive in infrared as well as Raman spectroscopy [14–16] *e.g.* when the double exclusion rule does not work.

2. Experimental

2.1 Synthesis of the oximino-compounds

The (*E*)-2 cyanoethylester-2-oxime needed for the present work has been synthesized with high yield by nitrosation reaction of the very reactive methylene group of ethyl cyanoacetate according to Conrad's procedure [17] by slowly dropping of a saturated solution of $NaNO_2$ into the reaction mixture of the cyanoester and glacial acetic acid. The temperature of the reaction had to be kept all times between −5 and 0 °C. An orange solid being the crude product obtained in the reaction was filtered off next day, made acidic to pH = 2 and after refrigeration it was filtered again. The (*E*)-2 cyanoethylester-2 oxime was then recrystallized from aqueous ethanol and when dry, it was again recrystallized twice from dichloromethane. Thus obtained (*E*)-2 cyanoethylester-2-oxime is very pure for spectroscopic measurements. 2-deuterated analogue of the 2-oxime was obtained after several crystallizations of 2-oxime in D_2O.

2.2 IINS measurements and computational details

The IINS spectra and simultaneously neutron powder diffraction (NPD) were measured at the inverted geometry time-of-flight spectrometer NERA [18,19] at the high-flux pulsed reactor IBR-2 in the Joint Institute for Nuclear Research in Dubna. The sample was mounted into a thin walled aluminum container ($165 \times 65 \times 1$ mm^3) at room temperature. The sample holder was then placed in the top-loaded neutron cryostat cooled with a helium refrigerator. Sample temperature could be changed within the range 20–300 K and stabilized with ±0.5 K accuracy at any chosen value. Within the energy transfer 5–100 meV the resolution of the NERA spectrometer is about 2–3% [20]. More details connected with neutron experiments, one can find in Supplement.

The neutron scattering intensities of 2-oxime were calculated by the α-CLIMAX program [21], using output values of atomic displacements and normal modes frequencies from the Gaussian 03 [22]. The IINS spectra of investigated molecular clusters (dimers) were calculated as a convolution of calculated neutron scattering intensities with the resolution function of the NERA-PR spectrometer [20]. Finally, the experimental and calculated time – of-flight IINS spectra were transformed in one-phonon

scattering approximation to the amplitude weighted density of vibrational states – $G(\upsilon)$. Such procedure allows us to compare the experimental and calculated INS vibrational spectra in a convenient energy transfer scale.

All calculations were carried out using the Gaussian'03 program [22]. Monomeric and dimeric structures of the studied compound were calculated using the DFT (density functional theory) approach. A series of geometry optimizations and vibrational frequency calculations were performed to characterize the key stationary points on the potential energy surface (PES) for the monomer. Geometry and frequency calculations were also executed for the dimer, starting from available crystallographic data [4]. Standard B3LYP functional (connection of Becke and Lee–Yang–Parr functionals) was used [28]. For results accuracy comparison, the PM3 semiempirical method [22] was employed for dimer calculations. Two basis sets were chosen for calculations, the 6-311++G(d,p) basis set [29] was used for the (*E*)-2-hydroxyimino-2-cyanoacetic acid ethyl ester monomer while calculations for the dimer (due to its size) were performed with lower 6-31* basis set [30].

Semiempirical methods are based on the classical Hartree–Fock scheme in which some integrals are parametrized, not calculated in a normal way [31]. In contrary the DFT theory is based on the Hohenberg–Kohn theorem and Kohn–Sham equations [32]. In the last two decades DFT has emerged as a practical and versatile tool to obtain accurate information about chemical systems. The popularity of DFT methods is based on the fact that they include a big part of electron correlation effects. That's why DFT methods achieve significantly greater accuracy that Hartree–Fock theory with more or less the same time of computations.

3. Results

The experimental IINS spectra of 2-oxime, obtained at different temperatures in this work, are presented in Figs. 2 and 3, respectively.

In the IINS spectra at the incident neutrons wave length of 0.4 nm one can see an elastic peak. Below 0.4 nm, *i.e.* in the region 0.05–0.4 nm there is an inelastic part of the spectra. One can distinguish here the acoustic branch and optical one. An energy gap is seen at 0.188 nm. An intensive band is seen at 0.15 nm in the low temperature IINS spectra.

Sharp peaks observed on the IINS spectrum obtained at $T = 20$ K suggest that vibrations in crystals can be treated as harmonic.

Thus the function $G(\upsilon)$ may be calculated assuming a one phonon mechanism [23] for the scattering process according to the formula:

$$\left(\frac{\mathrm{d}^2\sigma}{\mathrm{d}\Omega\,\mathrm{d}\upsilon}\right)_{\mathrm{inc}} = \frac{\boldsymbol{k_1}}{\boldsymbol{k_0}}\frac{hk^2}{8\pi^2 M\upsilon}(b^{\mathrm{inc}})^2\frac{\exp(-2W(\vec{k}))}{\exp\left(\frac{h\upsilon}{k_{\mathrm{B}}T}\right)-1}G(\upsilon)$$

where $\frac{\mathrm{d}^2\sigma}{\mathrm{d}\Omega\,\mathrm{d}E'}$ is the cross-section for incoherent neutron scattering, $\vec{k} = \vec{k}_0 - \vec{k}_1$ the momentum transfer, $h\omega = (h^2/2M)(k_0^2 - k_1^2)$ the energy transfer, $W(\vec{k})$ – the Debye–Waller factor, and $G(\upsilon)$ – the phonon density of states function.

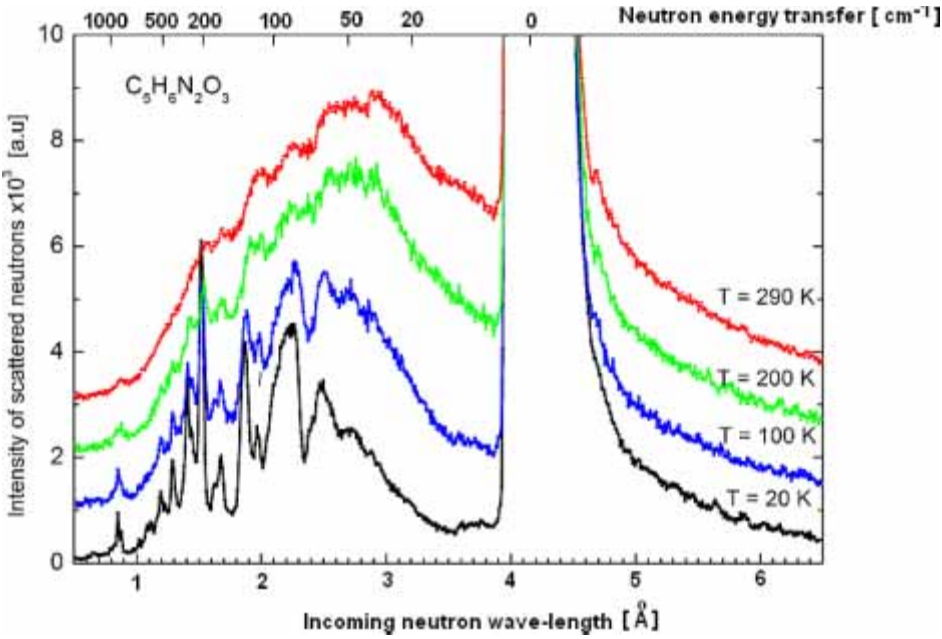

Fig. 2. The IINS spectrum of the (*E*)-2-cyanoethylesters-2-oxime in the temperature region from 20 K to 290 K For changing *x*-axis units into energy one must use the well-known dependence: $\lambda = 9.05\, E^{-0.5}$ (Å), where λ means the neutron wavelength and E the neutron energy (meV) corresponding to λ.

The IINS bands are getting broader when increasing temperature, they are getting smeared. This behavior is typical for IINS of crystals and it corresponds to increase of unharmonic character of vibrational modes with increasing temperature. At the room temperature one can not see even any energy gap between the lattice mode and internal ones. Figure 3 shows how temperature influences on the phonon density of state spectra $G(\upsilon)$ of 2-oxime obtained from IINS in one phonon scattering approximation. In order to assign reliable all experimental frequencies (*vide* Table 3) (20 K) of the $G(\upsilon)$ spectrum (Fig. 3) of the 2-oxime, the structure of isolated molecule and for dimer bonded by hydrogen bridge bond [4,10,24–27] was optimized. Then the frequencies of normal modes were calculated using methods described in the chapter *Computational details*.

The frequencies of internal modes were calculated for (*E*)-2-cyanoethyl ester-2-oxime molecule and the same molecule but with OH group isotope substituted by the OD group.

It is known that isolated 2-oxime molecule may obtain different conformations cis or trans as shown Fig. 4. The Table 1 collect their energies of formation. The lowest energy one is conformation 1. The low energetic conformations are presented on Fig. 4a–f.

From Table 1 we can readily see that conformation 1 of the (*E*)-2-cyanoethylester 2-oxime molecule is predominant. In Table 2 we can see a comparison between calculated data of bond length and angles for the conformation 1 and structural X-ray data. It should be noted that conformations 1, 2, 9 correspond to the *S-cis* conformations men-

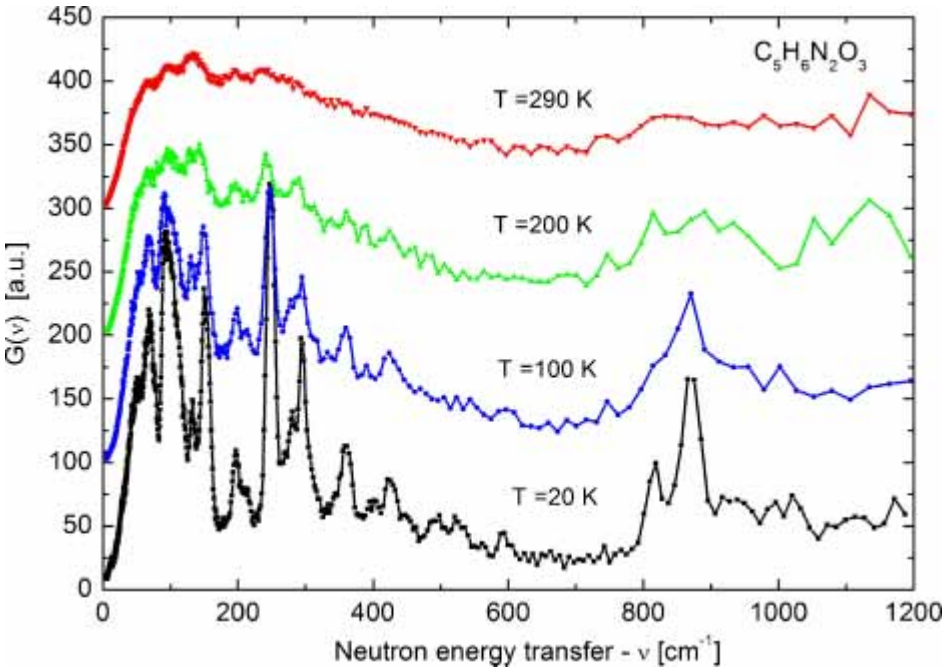

Fig. 3. Phonon density of states $G(\upsilon)$ for of the (*E*)-2-cyanoethylesters-2-oxime at variable temperatures.

Table 1. The most probable conformations of the (*E*)-2-cyanoethylesters-2-oxime molecule obtained by theoretical calculations (B3LYP/6-311++G(d,p)), their energies [kJ/mol] and populations [%].

	Energy	Relative energy	Free energy	Population
Conf1	−529.39881171	0.00000	−529.32128	35.21
Conf2	−529.39233147	17.01388	−529.31519	0.56
Conf3	−529.39282101	15.72860	−529.31594	0.12
Conf4	−529.39843915	0.97815	−529.32124	33.85
Conf5	−529.38817324	27.93130		
Conf6	−529.38186644	44.48980		
Conf7	−529.38212772	43.80383		
Conf8	−529.38756703	29.52291		
Conf9	−529.39812401	1.80555	−529.32071	19.15
Conf10	−529.39812460	1.80402		
Conf11	−529.39777421	2.72396	−529.32023	11.62
Conf12	−529.39777397	2.72458		

tioned at the beginning of the article, whereas 3, 4, 11 correspond to the *S-trans* forms but all of them concern the configuration *E* (entgegen – from German) of the molecule.

In Fig. 5 we compare the $G_{exp}(\upsilon)$ spectrum at 20 K for normal (hydrogenous *i.e.* undeuterated) and deuterated 2-oxime as well as for dimer-OH and for the single

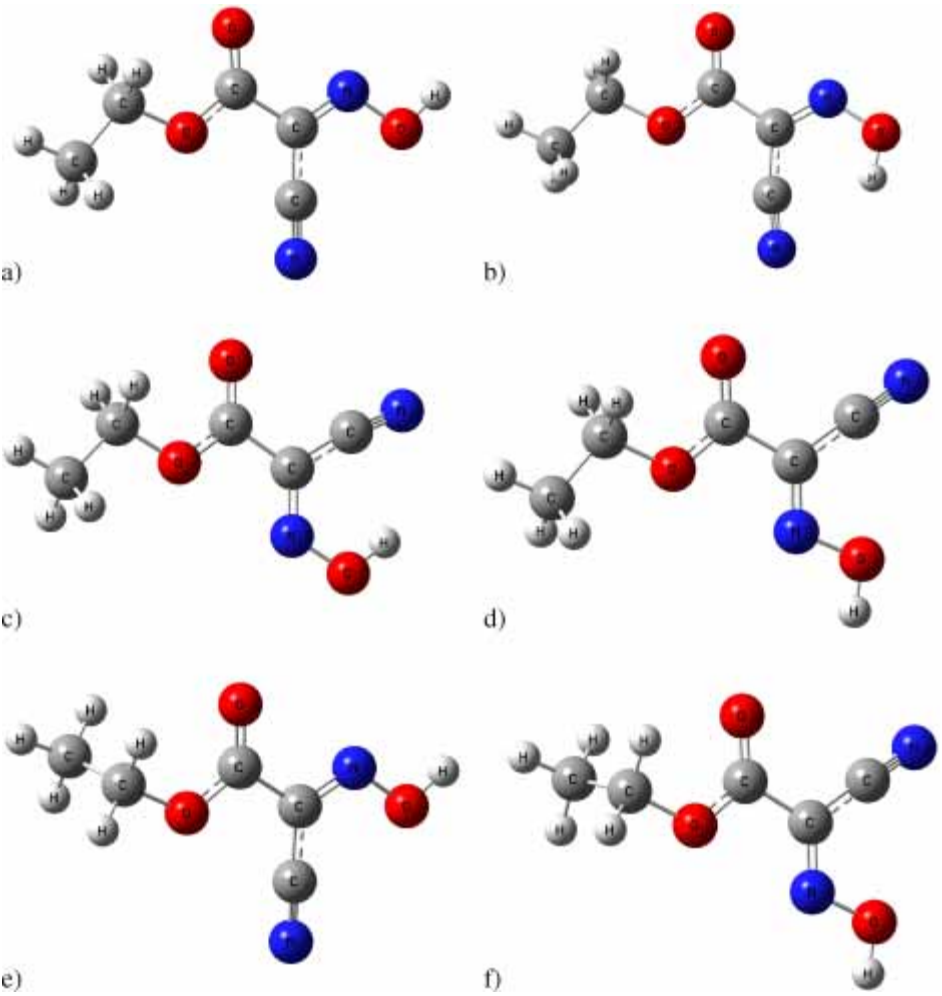

Fig. 4. (**a**) The molecule has the conformation 1 (S-cis) characterized by the lowest energy. In its deuterated form used in the present work, there is a deuterium atom instead of hydrogen atom in =N−O−H group of of the molecule. (**b**) Conformation 2 of (*E*)-2-cyanoethylester 2-oxime molecule (S-cis). (**c**) Conformation 3 of (*E*)-2-cyanoethylester 2-oxime molecule (S-trans). (**d**) Conformation 4 of 2(*E*)-2-cyanoethylester-oxime molecule (S-trans). (**e**) Conformation 9 of (*E*)-2-cyanoethylester 2-oxime molecule (S-cis). Atomic marking in the (*E*)-2-hydroxyimino-2-cyanoacetic acid ethyl ester molecule is presented. (**f**) Conformation 11 of (*E*)-2-cyanoethylester 2-oxime molecule (S-trans).

molecule. The spectra were calculated after transformation of theoretical frequencies received for the conformation 1 and for higher energetical conformations from Table 1 to the IINS spectrum and for the conformation of dimer (shown also in inserts of Fig. 5 and in Table 3).

In Fig. 5a experimental phonon density of state $G_{exp}(\upsilon)$ in the frequency region from very low till ca 1000 cm^{-1} can be observed, the resolution comparable with

Table 2. Comparison of X-ray data [4] for 2-oxime molecule with theoretical calculations for conformation1 performed by B3LYP/6-311++G(d,p) method, and the geometry of isolated molecule optimized by DFT/B3LYP/6-311G** and PM3 as well as for dimer optimized by B3LYP/6-31G* method.

Structural parameters	Data from [10] $T = 293$ K	Conformer I B3LYP/6-311++ G(d,p)	Optimised X-ray data B3LYP/6-311G**	Isolated molecule PM3	Isolated molecule B3LYP/6-311G**	Dimer B3LYP/6-31G* Proton donor (D)	Proton acceptor (A)
			Bond length [Å]				
C5–C4	1.445 1.536	1.5133	1.5133	1.51569	1.51591	1.51624	1.51464
C4–O3	1.475 1.504	1.4558	1.4558	1.43246	1.45182	1.44892	1.45960
O3–C3	1.298 1.328	1.3372	1.3372	1.35877	1.34089	1.34530	1.32667
C3–O2	1.262 1.152	1.2012	1.2012	1.21134	1.20781	1.20886	1.21878
C1–N1	1.139 1.149	1.1542	1.1542	1.15872	1.16226	1.16271	1.16210
C2–C1	1.428 1.409	1.4332	1.4333	1.42822	1.43642	1.43698	1.43400
C3–C2	1.485 1.516	1.5110	1.5110	1.50899	1.50796	1.50102	1.50217
C2–N2	1.253 1.317	1.2859	1.2859	1.29871	1.29187	1.29630	1.29198
N2–O1	1.392 1.307	1.3629	1.3630	1.37502	1.36635	1.34981	1.35441
O1–H1	0.849 0.850	0.9661	0.9661	0.95321	0.97272	0.98737	0.97481
C4–H		1.0191	1.0920	1.10624	1.09433	1.09459	1.09366
C4–H		1.0191	1.0920	1.10619	1.09432	1.09459	1.09365
C5–H	0.960	1.0918	1.0918	1.09803	1.09427	1.09441	1.09412
C5–H	0.959	1.0931	1.0932	1.09747	1.09427	1.09441	1.09412
C5–H	0.960	1.0918	1.0918	1.09801	1.09529	1.09539	1.09505
RMS	0.0622	0.0335	0.0314	0.0415	0.0357	0.0341	0.0346

Table 2. Continued.

Structural parameters	Data from [10] $T = 293$ K	Conformer I B3LYP/6-311++ G(d,p)	Optimised X-ray data B3LYP/6-311G**	Isolated molecule PM3	Isolated molecule B3LYP/6-311G**	Dimer B3LYP/6-31G* Proton donor (D)	Dimer B3LYP/6-31G* Proton acceptor (A)
			Internal angles [deg]				
H1 O1 N2	109.22 108.66	103.83	103.83	101.97	103.174	105.080	103.357
O1 N2 C2	115.30 107.18	113.23	113.23	119.66	112.661	112.934	113.950
N2 C2 C3	115.74 118.46	115.42	115.93	117.88	115.880	116.460	114.506
C2 C3 O3	105.34 114.68	109.73	109.72	111.90	109.798	109.917	111.198
O2 C3 O3	125.34 125.27	125.86	125.86	121.63	125.806	125.244	124.946
C3 O3 C4	114.07 116.98	116.67	116.67	118.15	116.034	115.898	116.716
O3 C4 C5	108.90 103.89	107.48	107.49	106.29	107.355	107.408	107.260
C2 C1 N1	177.21 177.81	179.38	179.31	179.45	179.811	178.800	179.864
N2 C2 C1	121.11 126.25	123.51	123.51	126.00	123.653	122.879	124.582
C1 C2 C3	123.16 115.29	120.56	120.56	116.12	120.467	120.651	120.912
C2 C3 O2	129.32 120.05	124.42	124.42	126.47	123.653	125.244	124.946
H–C4–H		108.02	108.10	107.92	107.833	107.699	108.108
H–C5–H	109.46	108.36	108.37	107.32	108.421	108.353	108.414
H–C5–H	109.46	108.36	108.37	107.58	108.434	108.431	108.542
H–C5–H	109.47	107.53	108.53	107.59	108.435	109.431	108.414
RMS	4.393	3.8597	3.8595	4.987	3.7458	3.7443	3.998
			Hydrogen bond				
O1–H	0.850 0.849					0.98737	
H···O2	1.851 1.854					1.81530	
O1···O2	2.690 2.701					2.80266	
O1–H···O2	169.13 174.85					179.606°	

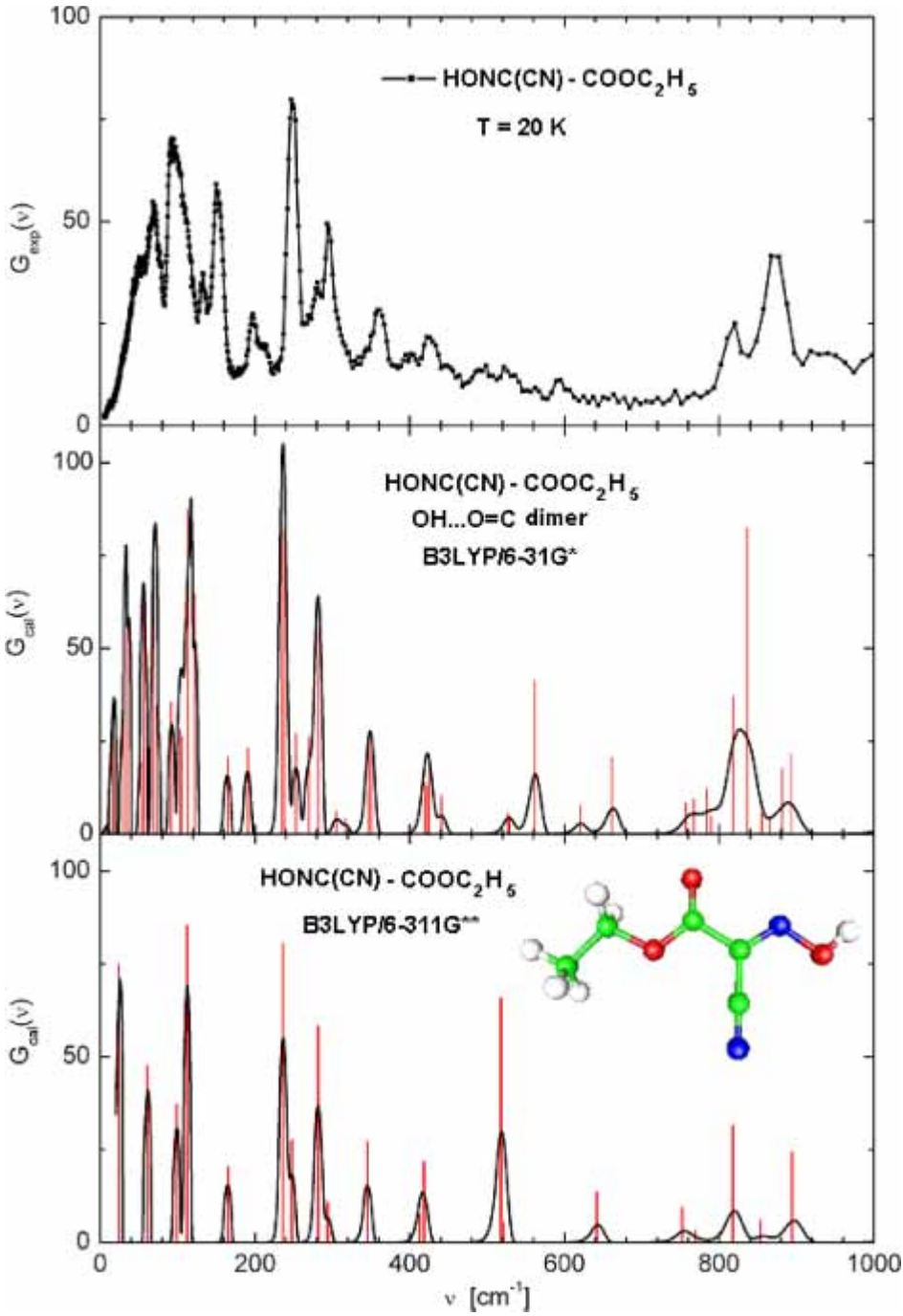

Fig. 5. (**a**) Experimental and calculated $G(\nu)$ for monomer and dimer O−H···O=C of (*E*)-2-cyanoethyl ester-2-oxime.

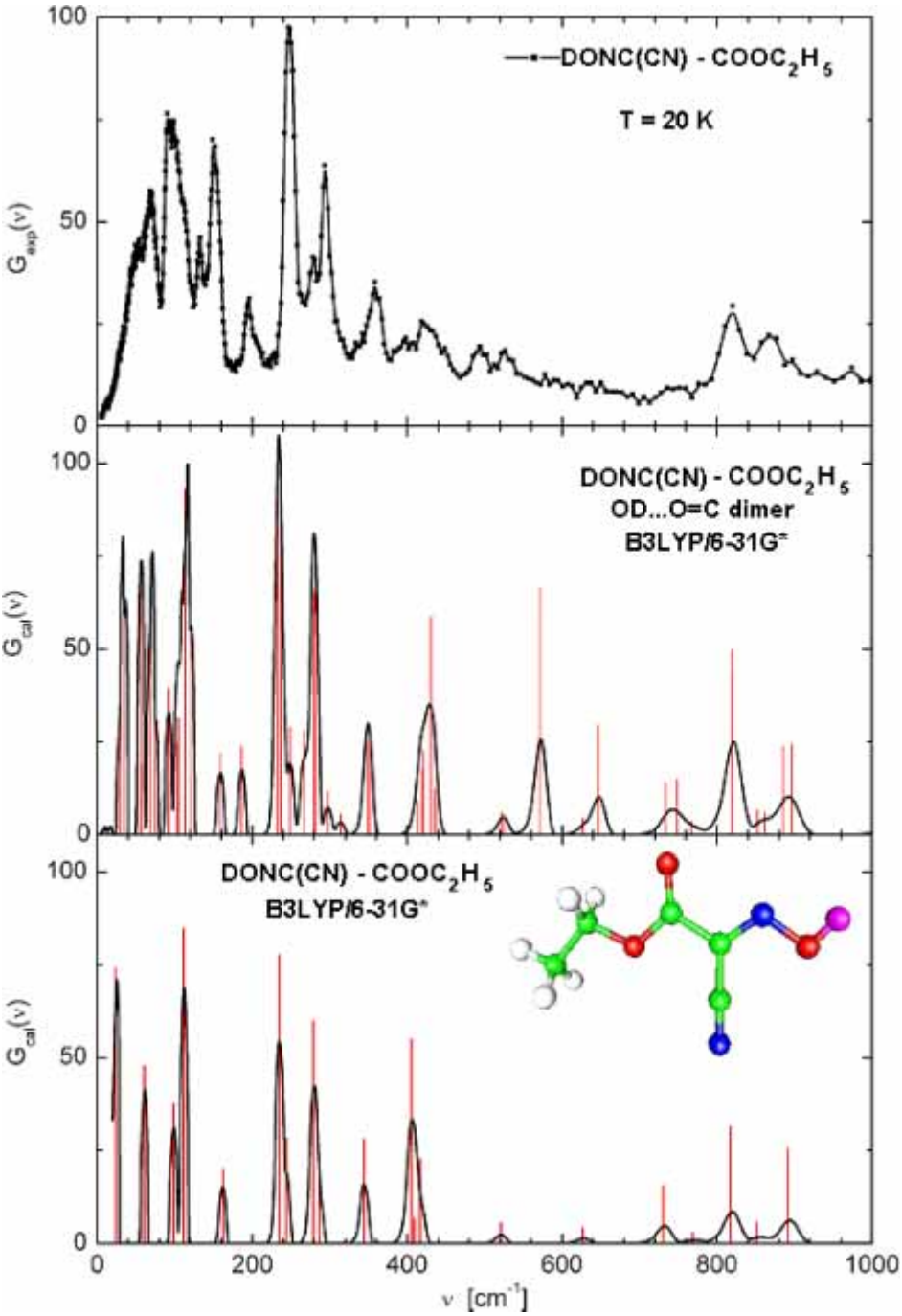

Fig. 5. (**b**) Experimental and calculated $G(\nu)$ for monomer and dimer O−D···O=C of (*E*)-2-cyanoethyl ester-2-oxime (deuterated).

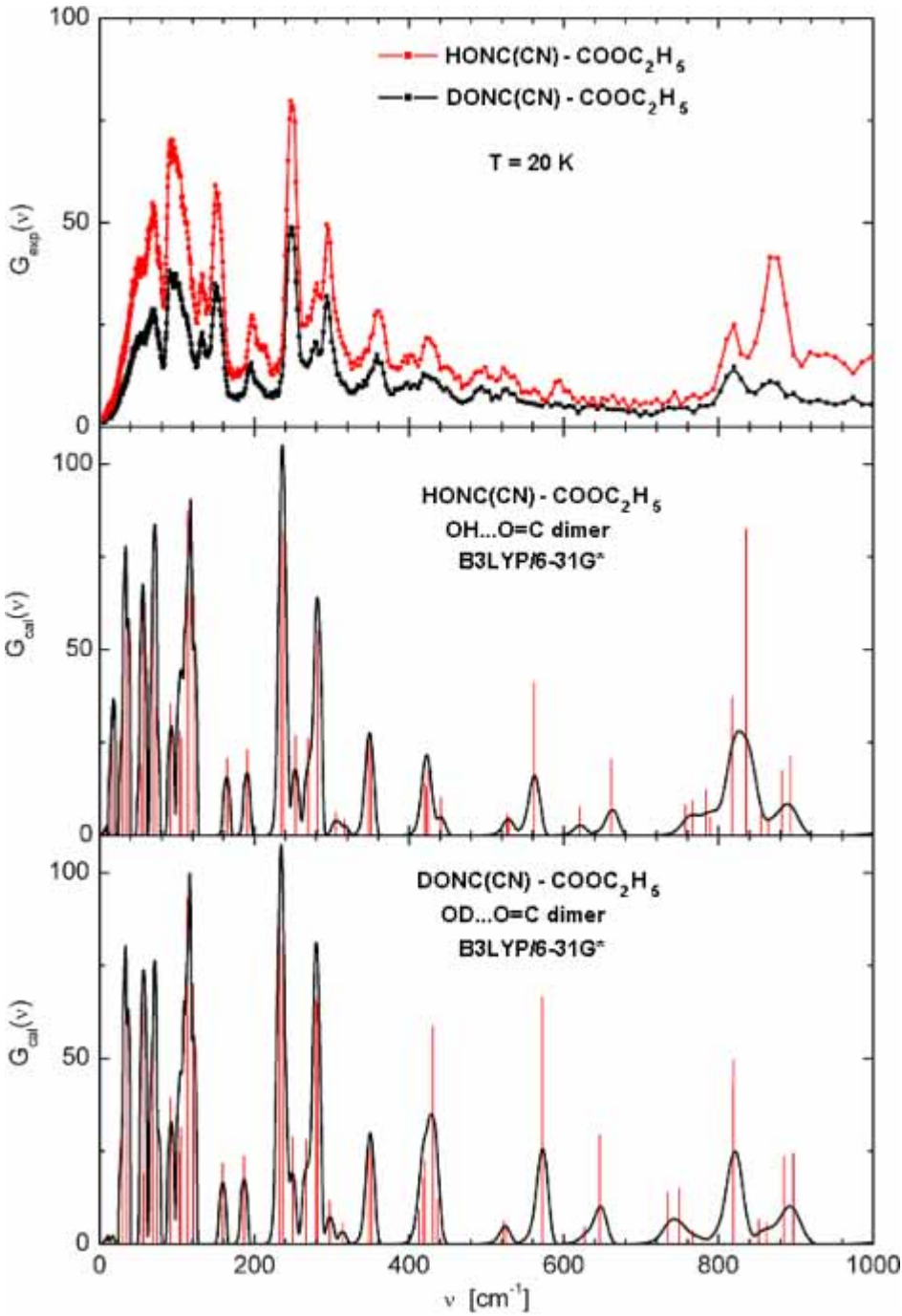

Fig. 5. (**c**) Experimental and calculated $G(\nu)$ for dimer ···O−H···O=C of (*E*)-2-cyanoethyl ester-2-oxime and dimer O−D···O=C of (*E*)-2-cyanoethyl ester-2-oxime.

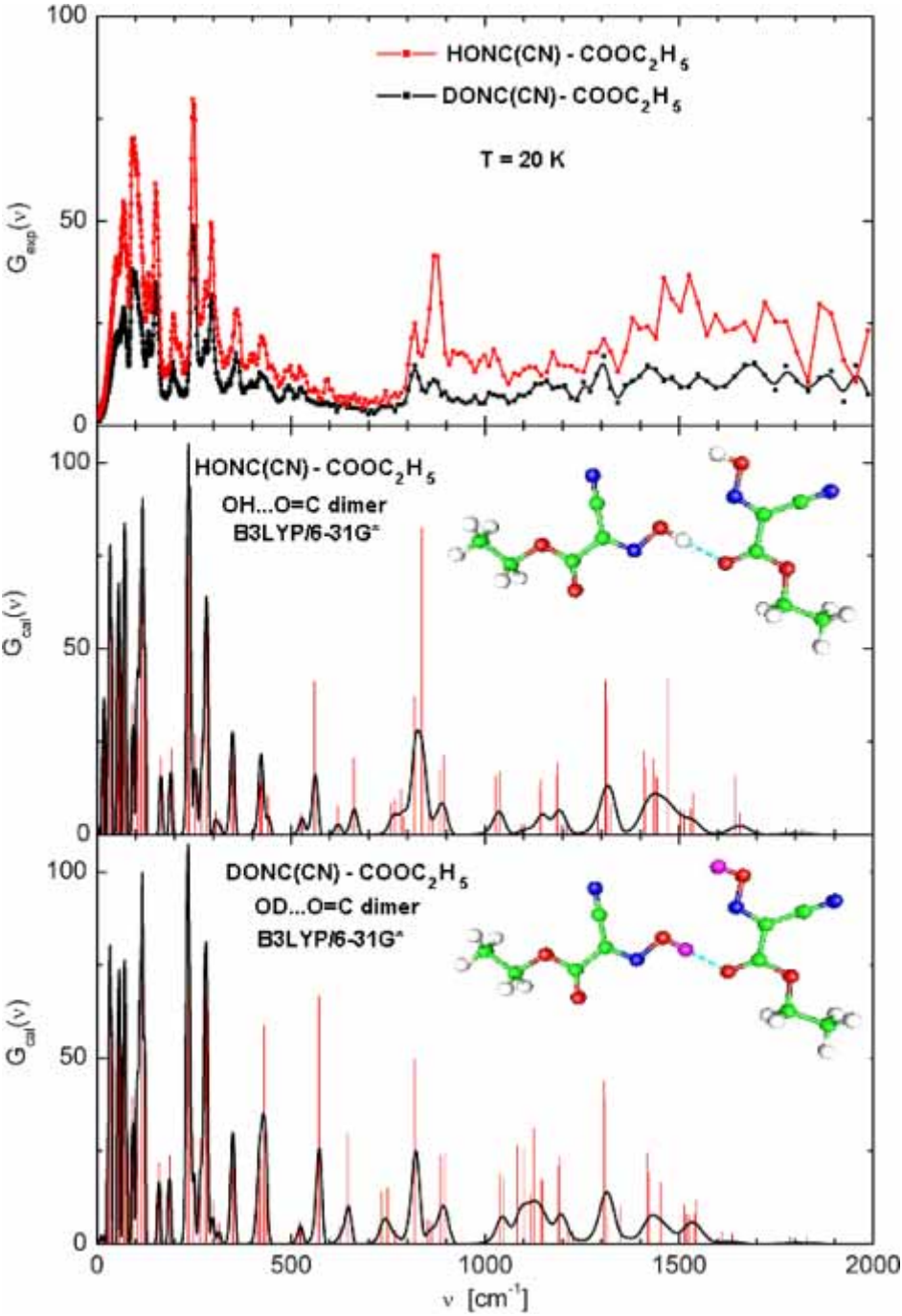

Fig. 5. (**d**) INS spectra for undeuterated and deuterated substance in the upper part of the diagram. In the lower part there is the simulated IINS by using of the theoretical frequencies for dimers in the frequency range up to 2000 cm^{-1}.

Table 3. The presented theoretical results concern the signed conformations of the molecule (characterised by the lowest energy (conformation1))and the low energetic conformation of dimer. The spectra are shown in the low frequency region. Atomic numbering (Fig. 1) in the (*E*)-2-hydroxyimino-2-cyanoacetic acid ethyl ester molecule as in [4] and used by us in the table; χ – means torsion out of plane, λ – bending of the hydrogen bond bridge, δ – deformation in plane, ρ – deformation out of plane, γ – out of plane motion of hydrogen bond, ν – stretching.

Frequencies of normal modes in [cm^{-1}]									
Given from the experimental data			Calculated by quantum chemical methods and proposed assignment of each band						
$G(\upsilon)$ in OH 20 K	IR in OH 16 K	Raman in OH $T = 293$ K	$G(\upsilon)$ in OD 20 K	DFT/ isolated molecule B3LYP/6-311++G (d,p)	DFT/ isolated molecule B3LYP/ 6-311/G**	DFT frequency/ dimer (A–H···B) B3LYP/6-31G* A	DFT frequency/ dimer (A–H···B) B3LYP/6-31G* B	Predominant assignment Atoms notation as in [4], see Fig. 1	PM3 isolated molecule	PM3-assignment when PED > 6% Atoms notation as in [4], see Fig. 1
						6.5	13.9	λ [O1–HO2]		
				33.01	24.2	15.7	29.7	λ [O1–HO2]	19.9	χ [C3–C2] 47% χ [C2–N2] 42%
49.5			52.7	67.1	60.9	35.7	56.4	ρ [C3–O2HO1] ρ [O3–C4–C5]	61.1	χ [O3–C3] 53% χ [O3–C3] 20% χ [C2–N2] 9%
68.2			69.2	98.9	98.9	57.7	69.1	χ [O3–C3] χ [C3–C2]	81.9	χ [O3–C3] 30% χ [O3–C3] 23% χ [C3–C2] 20% χ [C5–C4] 8%
93.7		118	93.7	113.2	112.5	74.5	92.3	ρ [C5–C4–O3] ρ [C3–O3–C4]	102.2	χ [C2–N2] 22% ρ [C3–C2–C1] 21% δ [O3–C3–C2] 18% δ [C4–O3–C3] 14% δ [C2–C3–O2] 8%

Table 3. Continued.

Frequencies of normal modes in [cm^{-1}]										
Given from the experimental data				Calculated by quantum chemical methods and proposed assignment of each band						
$G(\upsilon)$ in OH 20 K	IR in OH 16 K	Raman in OH $T = 293$ K	$G(\upsilon)$ in OD 20 K	DFT/ isolated molecule B3LYP/6-311++G (d,p)	DFT/ isolated molecule B3LYP/ 6-311/G**	DFT frequency/ dimer (A–H···B) B3LYP/6-31G* A	DFT frequency/ dimer (A–H···B) B3LYP/6-31G* B	Predominant assignment Atoms notation as in [4], see Fig. 1	PM3 isolated molecule	PM3-assignment when PED > 6% Atoms notation as in [4], see Fig. 1
132.8	128	137	132.8	166.5	164.8	103.9	104.7	δ [C3–C2–C1] δ [C1–C2–N2] σ (O1–H···O2)	148.1	λ [C2–C1–N1] 29% χ [C5–C4] 26% δ [C3–C2–C1] 16% δ [C1–C2–N2] 15%
150.9 178.5			150.9	233.6	236.3	113.9	121.1	χ [C4–C5] χ [C3–O3] ρ [C3–O3–C4]	163.2	χ [C5–C4] 60% δ [C2–N2–O1] 9% δ [C1–C2–N2] 9% λ [C2–C1–N1] 7% δ [C3–C2–N2] 5%
196.1	190	186.5	194.0	247.6	247.6	162.1	189.6	δ [N1–C1–C2] δ [C2–N2–O1]	209.8	δ [C3–C2–N2] 24% χ [O3–C3] 17%
212.5	205		201					δ [C3–C2–C1] σ [O1–H···O2]		ρ [O3–C3–C2] 17% δ [C2–N2–O1] 14% δ [C3–C2–C1] 9%
248.8	241		246.6	280.0	281.8	234.3	237.7	χ [C4–C5] ρ [C3–C2–C1]	246.7	χ [C2–N2] 32% δ [C4–O3–C3] 28% ρ [C3–C2–C1] 13% δ [C5–C4–O3] 12%

Table 3. Continued.

Frequencies of normal modes in [cm^{-1}]										
Given from the experimental data			Calculated by quantum chemical methods and proposed assignment of each band							
$G(\upsilon)$ in OH 20 K	IR in OH 16 K	Raman in OH $T = 293$ K	$G(\upsilon)$ in OD 20 K	DFT/ isolated molecule B3LYP/6-311++G (d,p)	DFT/ isolated molecule B3LYP/ 6-311/G**	DFT frequency/ dimer (A–H···B) B3LYP/6-31G* A	DFT frequency/ dimer (A–H···B) B3LYP/6-31G* B	Predominant assignment Atoms notation as in [4], see Fig. 1	PM3 isolated molecule	PM3-assignment when PED > 6% Atoms notation as in [4], see Fig. 1
279.0	270		281.1	293.4	293.8	252.1	271.0	δ [C4–O3–C3] δ [C5–C4–O3] δ [C2–N2–O1] σ [O1–H···O2] δ [N2–C2–C3]	283.1	χ [N2–O1] 42% λ [C2–C1–N1] 25% χ [C2–N2] 1716% ρ [C3–C2–C1]11%
293.8	306	308.5	293.6	342.6	345.3	281.5	281.7	ρ [C3–O3–C4] ρ [C5–C4–O3] ρ [C3–C2–C1]	366.7	χ [N2–O1] 64% λ [C2–C1–N1] 22%
334				412.1	412.6	302.1	315.2	ρ [O1–N2–C2] ρ [C2–C1–N1] γ [O1–H···O2]	375.6	δ [C5–C4–O3] 34% δ [O3–C3–O2] 24% δ [C2–C3–O2] 8% δ [C2–N2–O1] 8%
358.7	354 392	362	358.5.	421.1	418.3	348.6	352.4	δ [C3–O3–C4] δ [C2–N2–O1] δ [C5–C4–O3] σ [O–H···O]	385.0	δ [C2–N2–O1] 22% δ [C4–O3–C3] 19% λ [C2–C1–N1] 17% ν [C3–C2] 13% δ [O3–C3–C2] 6%

Table 3. Continued.

Frequencies of normal modes in [cm^{-1}]										
Given from the experimental data				Calculated by quantum chemical methods and proposed assignment of each band						
$G(\upsilon)$ in OH 20 K	IR in OH 16 K	Raman in OH $T = 293$ K	$G(\upsilon)$ in OD 20 K	DFT/ isolated molecule B3LYP/6-311++G (d,p)	DFT/ isolated molecule B3LYP/ 6-311/G**	DFT frequency/ dimer (A–H···B) B3LYP/6-31G* A	DFT frequency/ dimer (A–H···B) B3LYP/6-31G* B	Predominant assignment Atoms notation as in [4], see Fig. 1	PM3 isolated molecule	PM3-assignment when PED > 6% Atoms notation as in [4], see Fig. 1
424		418	419.0	514.0	518.0	416.5	420.4	δ [C2–N2–O1] λ [C2–C1–N1] δ [C5–C4–O3] σ [O1–H···O2]	439.3	δ [C2–N2–O1] 20% λ [C2–C1–N1] 13% δ [C5–C4–O3] 13% δ [O3–C3–C2] 10% λ [C2–C1–N1] 10%
448	435 447					422.6	441.0	δ [C2–N2–O1] δ [C5–C4–O3] δ [C2–C3–O2]	496.7	λ [C2–C1–N1] 46% ρ [O3–C3–C2] 9% ν [C3–C2] 9%
488			495.6	522.4	521.2			σ [O1–H···O2] δ [N1–C1–C2]		δ [C2–N2–O1] 6% δ [C4–O3–C3] 6%
522.6	514.5	519	531.7	639.1	642.0	522.7	525.4	δ [C2–C1–N1] δ [O3–C3–C2] δ [C3–C2–N2] σ [O1–H···O2]	685.9	ρ [O3–C3–C2] 60% δ [C3–C2–N2] 7% ν [N2–O1] 5% ν [C2–C1] 5%
564		583		751.4	752.2	550.5	615.1	ρ [N1–C1–C2] ρ [C3–C2–N2] ρ [O1–N2–C2] γ [O1–H···O2]	731.8	ρ [O3–C3–C2] 16% δ [C2–N2–O1] 11% λ [C2–C1–N1] 11% δ [C4–O3–C3] 11% δ [C3–C2–C1] 9%

Table 3. Continued.

Frequencies of normal modes in [cm^{-1}]										
Given from the experimental data			Calculated by quantum chemical methods and proposed assignment of each band							
$G(\upsilon)$ in OH 20 K	IR in OH 16 K	Raman in OH $T = 293$ K	$G(\upsilon)$ in OD 20 K	DFT/ isolated molecule B3LYP/6-311++G (d,p)	DFT/ isolated molecule B3LYP/ 6-311/G**	DFT frequency/ dimer (A–H···B) B3LYP/6-31G* A	DFT frequency/ dimer (A–H···B) B3LYP/6-31G* B	Predominant assignment Atoms notation as in [4], see Fig. 1	PM3 isolated molecule	PM3-assignment when PED > 6% Atoms notation as in [4], see Fig. 1
592			579.1	792.0	769.2	650.9	756.2	δ [C2–N2–O1] δ [C3–C2–C1] δ [N1–C1–C2] δ [O3–C3–O2] γ [O1–H···O2]	745.0	ρ [C3–C2–C1] 47% λ [C2–C1–N1] 18% δ [C2–C3–O2] 8% δ [C4–O3–C3] 5%
652	754.0	752	639.7 735.4	816.1	817.7	763.8	766.1	δ [C2–N2–O1] δ [O1–HO2] δ [N1–C1–C2] δ [C2–C3–O2] γ [O1–H···O2]	806.9	δ [C5–C4–H12] 21% δ [C5–C4–H13] 21% δ [C4–C5–H16] 16% δ [C4–C5–H14] 16% δ [O3–C4–H12] 11%
768.2	768.3	765.5		850.4	853.0	767.5	819.1	δ [C4–C5–H1] δ [C5–C4–H1]	851.5	ν [C2–C1] 24% ν [C3–C2] 15% ν [N2–O1] 10% δ [C4–O3–C3] 10% δ [C2–N2–O1] 8%
820	848.0			881.3	894.2	819.4	832.6	γ [O1–H···O2] ρ [C3–C2–N2]	918.7	δ [C4–C5–H15] 41% ν [C4–O3] 24% δ [C4–C5–H14] 8% δ [C4–C5–H16] 7% ν [N2–O1] 6%

Table 3. Continued.

Frequencies of normal modes in [cm^{-1}]										
Given from the experimental data			Calculated by quantum chemical methods and proposed assignment of each band							
$G(\upsilon)$ in OH 20 K	IR in OH 16 K	Raman in OH $T = 293$ K	$G(\upsilon)$ in OD 20 K	DFT/ isolated molecule B3LYP/6-311++G (d,p)	DFT/ isolated molecule B3LYP/ 6-311/G**	DFT frequency/ dimer (A–H···B) B3LYP/6-31G* A	DFT frequency/ dimer (A–H···B) B3LYP/6-31G* B	Predominant assignment Atoms notation as in [4], see Fig. 1	PM3 isolated molecule	PM3-assignment when PED > 6% Atoms notation as in [4], see Fig. 1
872		858	863.0	1024.6	1039.9	853.4	863.7	ν [C2–C3] ν [C1–C2] δ [C3–O3–C4] δ [O2–C3–O3] δ [C2–C3–O3] σ [O1–H–O2]	1004.7	δ [O3–C4–H12] 35% δ [O3–C4–H13] 34% δ [C4–C5–H16] 11% δ [C4–C5–H14] 10%
940				1059.9	1081.6	887.8	898.8	ν [O3–C4] ν [C4–C5] δ [C2–C3–O2] δ [O3–C3–C2] ν [N2–O1]	1021.0	ν [N2–O1] 68% δ [N2–O1–H] 9% ν [C3–C2] 6%
997			1089.6			1036.2	1047.3	ν [C4–C5] ν [O3–C4] ν [O1–N2] δ [C5–C4–O3]	1079.3	ν [C4–O3] 33% ν [C5–C4] 22% δ [O3–C4–H] 12% δ [O3–C4–H] 11% δ [C5–C4–H] 6%
1073	1068.5	1062.5				1106.7	1114.0	ν [O1–N2] ν [O3–C4] ν [O3–C3] δ [C3–O3–C4] δ [C4–C5–H]	1096.3	δ [C5–C4–H] 27% δ [C5–C4–H] 27% δ [C4–C5–H] 19% δ [C4–C5–H] 19%

Table 3. Continued.

Frequencies of normal modes in [cm^{-1}]										
Given from the experimental data				Calculated by quantum chemical methods and proposed assignment of each band						
$G(\upsilon)$ in OH 20 K	IR in OH 16 K	Raman in OH $T = 293$ K	$G(\upsilon)$ in OD 20 K	DFT/ isolated molecule B3LYP/6-311++G (d,p)	DFT/ isolated molecule B3LYP/ 6-311/G**	DFT frequency/ dimer (A–H···B) B3LYP/6-31G* A	DFT frequency/ dimer (A–H···B) B3LYP/6-31G* B	Predominant assignment Atoms notation as in [4], see Fig. 1	PM3 isolated molecule	PM3-assignment when PED > 6% Atoms notation as in [4], see Fig. 1
1115		1114		1133.1 1176.0	1145.6	1145.6	1147.0	δ [C4–C5–H] δ [O3–C4–C5] δ[C3–O3–C4]	1127.8	ν [C5–C4] 38% ν [C4–O3] 13% δ [C4–O3–C3] 8% δ [C5–C4–O3] 7% δ [H–C4–H] 7%
1173	1186.9	1186.5	1158	1185.6	1191.0	1184.5	1192.1	δ [O3–C4–H] δ [C4–C5–H]	1257.2	ν [O3–C3] 28% ν [C2–C1] 25%
				1277.1	1200.2	1209.1	1218.2	ν [O3–C3] ν [C1–C2] δ [C3–C2–N2] δ [O1–N2–C2]	1283.7	ν [C4–O3] 32% ν [O3–C3] 12% δ [O3–C4–H] 10% δ [O3–C4–H] 9% δ [C4–C5–H] 7%
		1278		1299.0	1303.0	1307	1309	δ [O3–C4–H] δ [C4–C5–H] δ [C5–C4–H]	1316.5	δ [H12–C4–H] 54% ν [C4–O3] 6% δ [C4–C5–H] 5% δ [C4–C5–H] 5% δ [H–C5–H] 5.31%
	1314.8	1315		1392.9	1308.0	1309.3	1340.0	δ [N2–O1–H] δ [O3–C4–H] ν [O3–C3]	1351.0	δ [H–C5–H] 48% δ [H–C5–H] 48%

Table 3. Continued.

Frequencies of normal modes in [cm^{-1}]										
Given from the experimental data				Calculated by quantum chemical methods and proposed assignment of each band						
$G(\upsilon)$ in OH 20 K	IR in OH 16 K	Raman in OH $T = 293$ K	$G(\upsilon)$ in OD 20 K	DFT/ isolated molecule B3LYP/6-311++G (d,p)	DFT/ isolated molecule B3LYP/ 6-311/G**	DFT frequency/ dimer (A–H···B) B3LYP/6-31G* A	B	Predominant assignment Atoms notation as in [4], see Fig. 1	PM3 isolated molecule	PM3-assignment when PED > 6% Atoms notation as in [4], see Fig. 1
	1371.3	1370	1306	1404.3	1411.1	1415.4	1416.6	δ [N2–O1–H] δ [O3–C4–H] δ [C4–C5–H]	1358.3	δ [H–C5–H] 60% δ [H–C5–H] 18% δ [H–C5–H] 17%
	1433.7		1424.3 1548	1429.5	1428	1436.8	1452.9	δ [O1–HO]		
		1428.5							1384.1	ν [C5–C4] 26% δ [H–C5–H] 8% δ [H–C4–H] 8% δ [C4–C5–H] 7% δ [C4–C5–H] 7%
1461	1471.6	1455		1486.1	1451.7	1454.4	1472.7	δ [O1–H···O2]	1406.5	ν [C3–C2] 30% ν [O3–C3] 29% ν [C2–C1] 11%
		1470		1498.3	1515.5	1514.5	1516.1	δ [C4–C5–H]	1491.3	δ [N2–O1–H] 82% ν [C2–N2] 7%
1524				1517.2	1543.3	1524.6	1526.1	δ [H–C5–H] δ [H–C4–H]		
	1582.9	1580	1695	1646.0	1660.5	1540.5	1544.8	δ [H–C5–H] δ [H–C4–H] δ [O1–H···O2]	1853.9	ν [C2–N2] 79% δ [N2–O1–H] 7% ν [C2–C1] 6%

Table 3. Continued.

Frequencies of normal modes in [cm^{-1}]										
Given from the experimental data				Calculated by quantum chemical methods and proposed assignment of each band						
$G(\upsilon)$ in OH 20 K	IR in OH 16 K	Raman in OH $T = 293$ K	$G(\upsilon)$ in OD 20 K	DFT/ isolated molecule B3LYP/6-311++G (d,p)	DFT/ isolated molecule B3LYP/ 6-311/G**	DFT frequency/ dimer (A–H···B) B3LYP/6-31G* A	DFT frequency/ dimer (A–H···B) B3LYP/6-31G* B	Predominant assignment Atoms notation as in [4], see Fig. 1	PM3 isolated molecule	PM3-assignment when PED > 6% Atoms notation as in [4], see Fig. 1
1600	1665.5			1807.5	1834.7	1648.2	1661.9	ν [N2–C2] δ [N2–O1–H] δ [C1–C2–C3] δ [O1–N2–C2]	1974.6	ν [C3–O2] 85% ν [C3–C2] 6%
1862	1728.2	1712.5	1892	2338.0	2351.4	1788.9	1830.3	ν [C3–O2] δ [O2–C3–C2] δ [O2–C3–O3] δ [N2–O1–H]	2472.8	ν [C1–N1] 84% ν [C2–C1] 15%
	2233.5	2232		3040.5	3065.9	2346.1	2355.1	ν [C1–N1]	2841.8	ν [C4–H] 50% ν [C4–H] 49%
	2850	2876		3058.0	3079.8	3064,5	3068.4	ν [C5–H]	2885.1	ν [C4–H] 50% ν [C4–H] 49%
	2989.6	2929		3095.6	3120.6	3076.9	3088.5	ν [C4–H]	2980.7	ν [C5–H] 51% ν [C5–H] 49%
	3134.9	2945		3107.4	3137.4	3116.7	3140.8	ν [C5–H] ν [C4–H]	2983.1	ν [C5–H] 67% ν [C5–H] 17% ν [C5–H] 15%
	3194.7	2977.5		3122.1	3149.1	3146.5	3154.0	ν [C5–H] ν [C4–H]	3067.4	ν [C5–H] 34.2% ν [C5–H] 34% ν [C5–H] 32%
	3400			3795.6	3725.9	3469.6	3702.3	ν [O1–H]	3778.8	ν [O1–H] 100%
RMS					83	40	46		269	

that obtained by optical spectroscopy techniques. For energy transfers greater than 1000 cm^{-1} the intensity of scattered neutrons decreased, therefore our assignment in Table 3 is mostly performed for frequencies up to *ca.* 1000 cm^{-1} and these results are trustworthy. Some peaks seen in the higher frequency region on the picture of phonon density function (Fig. 3) can be a result of scattered experimental points. In Table 3 the wave numbers of subsequent normal modes from optical spectroscopy are collected as well.

4. Discussion of results

4.1 Geometry of monomer and dimer of 2-oxime

The optimized molecular structure of 2-oxime dimer is the simplest step in reproduction of the real structure of this compound. Comparison of the geometric parameters of monomer and proton donor and proton acceptor in the 2-oxime dimer (Table 2) shows how formation of the hydrogen bond changes the geometry of proton donor and proton acceptor. The O−H···O hydrogen bond in the lowest energetically structure obtained in optimization is molecular one with the proton located at the proton donor. The O···O, OH and H···O bonds length equals to 2.802, 0.987, 1.815 Å respectively. The O−H···O angle is 176.6°.

Comparison of the geometric parameters from Table 2 shows shortening of the OH bond length if this group is used as a proton donor. The C=O bond length is also sensitive to the formation of the hydrogen bond and decreases in the proton donor molecule and elongates in proton acceptor. Other geometric parameters listed in Table 2 also undergo changes under the hydrogen bond formation. The C−C bond lengths are slightly elongated in proton donor (in the ethyl-group) and shortened in proton acceptor. Analogous changes are seen for the O−C−C angles which increase in the proton donor and decrease in proton acceptor.

The X-ray data taken at room temperature given the O(1)···O(2) distance are 2.690 and 2.701 Å, while calculated for dimer is 2.802 Å. The hydrogen bond is nearly linear, i.e the angle O(1)−H···O(2) is 179° for optimized structure, while 169 and 174° in the X-ray data [4]. The root mean square deviation (RMS) between the experimental bond length or angles X_i and the calculated ones $X_{i,\mathrm{cal}}$ by different quantum chemistry methods (QC), (DFT or PM3) was calculated according to the formula:

$$\mathrm{RMS} = \left[\frac{\Sigma(X_i - X_{i,\mathrm{cal}})^2}{n}\right]^{1/2}.$$

The RMS factors calculated for the structures optimized by different QC method of isolated molecule and for dimer are collected in Table 2. It takes the following values, which are close to each others: for isolated molecule 0.0314, 0.0415, 0.0357 Å; 4.0937, 4.987, 3.7458° and for dimer 0.0341, 0.0346 Å and 3.7443, 3.9979°, respectively.

4.2 Vibrational modes of 2-oxime monomer

The first step concerning the analysis of the experimental spectra of 2-oxime is investigation of the theoretical spectrum of its monomer and to make an assignment of the

most characteristic vibrations. The υ(OH) stretching vibration of free (hydroxylic) OH group in 2-oxime was located at 3725 cm^{-1}. δ(O1−H1) was assigned to the band at 1660.48 cm^{-1} but it participated also in the other bands at 1451.7, 1428, 1411.1, 1303.0, 1200.2, 1081.6 cm^{-1}. It was impossible to find a band assigned only to σ(O1−H1), γ(O1−H1) vibrations which participated in the bands at 164.8, 247.6, 345.3, 418.2, 521.2 σ(O1−H1), 236.3, 293.8, 518, 642, 769.2 cm^{-1} γ(O1−H1). For monomer of 2-oxime coupling of the proton vibrations with other molecular vibrations is well seen in the results of calculations showing frequencies of vibrations and kinds of vibrations contributing. We do not present an assignment for monomer in Table 3, but in Table 4. It is characteristic that both deformation vibrations do not appear as separate bands but are always coupled with other bonds. For example band at 164.8 cm^{-1} is coupled with torsion vibration out of plane of ethyl group and with bending vibration of C−C≡N group. Band at 247.6 cm^{-1} is coupled with bending vibration of ethyl and ethyl−O−C group, with deformation in plane of C−C≡N group. Also the stretching vibration of carbonyl group does not exist as separate band but is coupled with torsion vibration of ethyl group.

4.3 Vibrations of 2-oxime dimer

To analyze the vibrations of the 2-oxime dimer the theoretical spectrum of the dimer has been compared with the spectra of analogues deuterated in the −OH group.

Formation of the O−H···O hydrogen bond is reflected in the stretching vibration of the proton donor OH group which shifts from 3725.9 to 3469.6 cm^{-1}. The bands with participation of the in-plane bending vibrations δ for donor are shifted to higher frequencies from 1145.6, 1200.2, 1303.0, 1428, 1451.7 and 1660.5 cm^{-1} to 1218.2, 1340, 1416.6, 1472.7, 1544.8, 1661.9 cm^{-1}, respectively. Analogous vibrational modes with participation δ OH for proton acceptor are also different than those of monomer and shifted to 1209, 1309.3, 1415.4, 1454.4, 1540.5, 1648.2 cm^{-1}. σ(OH) for donor are shifted to higher frequencies from 164.8, 247.9, 345.3, 418.2, 521.1 cm^{-1} to 189.6, 271.0, 352.4, 420.4, 525.4 cm^{-1}, γ(OH) for donor are shifted to higher frequencies from 293.8, 518, 642, 769.2 cm^{-1} to 315.2, 615.1, 756.2, 832.6 cm^{-1}.

4.4 Experimental spectra

According to the formula for the $G(\nu)$ function, the intensity of neutron scattering is proportional to the square of atom displacement. The phonon density of states function of parent undeuterated oxime (Fig. 3) at various temperatures and undeuterated and deuterated ones (at 20 K) are shown in Fig. 5. The frequencies of the observed INS bands are collected in Table 3. Nine vibrational modes at 212.5, 448, 564, 592, 867.2, 937.5, 1461, 1600, 1862 cm^{-1} observed in undeuterated oxime were found to be absent for the deuterated sample of 2-oxime. Their predominant assignment we can find in Table 3. The mentioned modes observed in our IINS experiment are related to the vibrations of hydrogen bonds between hydrogen atom of the N−O···H group and oxygen atoms belonging to the ester carbonyl group of the neighboring molecule or to vibration of N−O−H group (which is not bonded in the considered dimerical molecule). From X-ray data of the (*E*)-2-cyanoethyl ester-2-oxime [4] we can see one single H-bond as

Table 4. Frequencies calculated (by B3LYP/6-311++G(d,p) method) for conformation 1 and PEDS greater than 10%.

Theor. freq. of $G(\upsilon)$	Assignment
3795.57	ν O1H1 100
3122.09	ν C(5)–H(5) 35% – ν C(5)–H(4) 35% – ν C(4)–H(3) 15% + νC(4)–H(2) 15%
3107.42	ν C(5)–H(6) 60% – ν C(5)–H(4) 19% – ν C(5)–H(5) 19%
3095.62	ν C(4)–H(2) 35% – ν C(4)– H(3) 35% – ν C(5)–H(5) 15% + ν C(5)–H(4) 15%
3057.96	ν C(4)–H(3) 49% + ν C(4)–H(2) 49%
3040.47	ν C(5)–C(4) 39% + ν C(5)–H(4) 30% + ν C(5)–H(5) 30%
2337.99	ν C(1)–N(1) 89% – ν C(2)–C(1) 11%
1807.51	ν C(3)–O(2) 79%
1645.99	ν N(2)–C(2) 72% – δN(2)–H(1)–O(1) 10%
1517.17	δ O(3)–C(5)–C(4) 72% δ H(5)–C(5) 14%
1498.27	δ H(5)–C(5) 48% – δH(3)–H(2)–C(4), O(3)–C(5)–C(4) 26% δ H(5)–C(5) 16%
1486.10	δC(5)–H(6) 68% – δ H(5)–C(5) 23%
1429.52	δ C(5)–H(6), C(4)–C(5) 53% + δO(3)–C(4), C(4)–C(5) 24% + ν C(4)–C(5) 13%
1404.29	δ C(5)–H(6), C(4)–C(5) 27% – δO(3)–C(4), C(4)C(5) 27% + δ N(2)–H(1)–O(1) 26%
1392.94	δN(2)–H(1)–O(1) 45% + δ O(3)–C(4), C(4)C(5) 31%
1299.0	δO(3)–C(4), C(4)–C(5) 88% + δ C(4)–C(5) 10%
1277.10	ν C(3)–O(3) 32% – ν C(2)–C(3) 27% + δ C(2)–O(2)–C(3) 11%
1185.55	ν C(2)–C(1) 20% – ν C(3)–O(3) 20% + δ N(2)–C(3)–O(2) 16% + δ C(2)–O(1)–N(2) 10%
1175.97	δ O(3)–C(4), C(4)–C(5) 50% – δ C(4)–C(5) 36%
1133.12	δ C(4)–C(5) 40% + ν C(4)–C(5) 22% + δO(3)–C(4)C(5) 13%
1059.93	ν C(1)–N(2) 56% + ν O(3)–C(4) 19%
1024.57	ν C(4)–C(5) 44% – ν O(3)–C(4) 20%
881.34	ν O(3)–C(4) 41% + δ C(4)–C(5)–H(6) 21%
850.42	δ O(2)–C(3)–O(3) 29% – δ C(3)–O(3)–C(4) 15% + ν C(2)–C(1) 12%
816.09	δ O(3)–H(3)–C(4) 39% + δ H(4)–C(4)–C(5) 35% – δ O(3)–H(3)–C(4) 13%
792.01	γ C(2)–C(3)–O(2) 59% + γ C(2)–C(1) 20%
751.43	δ O(1)–N(2)–C(3) 27% – δ C(3)–C(4) 23% – δ N(2)–C(3)–C(4) 21%
639.06	γ C(3)–C(2)–C(1) 23% – χ O(1)–N(2) 22% + χ N(2)–C(3) 20%
522.37	δ C(2)–C(1)–N(1) 16% – δ N(2)–C(2)–C(1) 16% + ν C(2)–C(1) 13%
513.98	χ O(1)–N(2) 77%
421.08	δ C(2)–C(3)–O(3) 23% + δ C(2)–C(1)–N(1) 22% – δ O(3)–C(4)–C(5) 22% – δ O(1)–N(2)–C(2) 18%
412.06	ν C(2)–C(3) 30% + δ O(1)–N(2)–C(2) 23% + δ C(2)–C(3)–O(2) 22%
342.57	δ C(4)–O(3)–C(5) 24% + δ C(3)–C(4)–O(3) 22% – δ C(2)–O(2)–C(3) 13%
293.43	χ C(2)–N(3) 49% – γ C(2)–C(1)–N(1) 42%
279.97	χ C(4)–C(5) 37% – χ C(3)–O(3) 26%
247.57	δ N(2)–C(3)–C(2) 38% – δ C(3)–O(3)–C(4) 22%
233.60	χ C(4)–C(5) 56%
166.47	δ C(2)–C(1)–N(1) 38% + δ N(2)–C(1)–C(2) 30%
113.23	χ C(3)–O(3) 62%
98.90	δ C(2)–C(3)–O(3) 28% – δ C(3)–O(3)–C(4) 24%
67.27	χ O(3)–C(4) 83% – χ C(2)–C(3) 13%
33.01	χ C(2)–C(3) 88%

hydrogen bridge between OH and oxygen atom of carbonyl group of neighboring. The length of the hydrogen bond O1−H1···O2 is equal 2.701 Å based on crystallographic data [4] whereas the corresponding length but of the distance O1−H1···N2 is equal to 3.236 Å in the same molecule of (*E*)-2 cyanoethylester-2-oxime. The angle between atoms: OHO = 174.86° in the first case and 114.23° in the second case (here between atoms: OHN).

Additionally, as we can see in Table 3 that nearly all vibrations associated with hydrogen bond bridge appear not as pure modes but they are accompanied by another vibrations. Typical vibrations related to the vibrations of hydrogen bonds between hydrogen atom of the hydroxyimino (N)−O···H group and oxygen atoms belonging to the ester carbonyl group C=O of the neighboring molecule are: σ(O−H···O): 132.8, 212.5, 279, 358.7, 424, 448, 522.6, 872, γ(O−H···O)-out-of-plane: 334, 564, 592, 745, 820 cm^{-1}, δ(N−OH···): 1461, 1600, 1862 cm^{-1}. The frequency at 405 cm^{-1} has been assigned as the out of plane (o.o.p.) ($\gamma_{O-D\cdots O}$) vibrational modes. It is present in the D sample and absent in the H-sample. The 937.5 cm^{-1} frequency could be responsible for torsion O−H (no peak in the D spectrum).

On the basis of [14,15] we can assign the modes at 150.9, 250, 293.8 cm^{-1} as ascribed to the libration of CH_3 group, out of plane vibrations of hydrogen of CH_2 group and of torsion of CH_3 respectively. It is in agreement with our assignment shown in Table 3 where at such the frequencies we observe out of plane torsion motions of the ethyl group.

The corresponding vibrations were observed in IINS spectra at 309 cm^{-1} (torsion of CH_3) in [15] for L and DL-valine, 228, 281 cm^{-1} [14] for L-isolueucine. A high intensity peak at 250 cm^{-1} suggests a large proton displacement in the CH_2 group. According to our assignment at the frequency we observe torsional motions of ethyl group.

The frequency 293.8 cm^{-1} describes out of plane skeletal motions and its result is a displacement of all protons. In methyl group there are 3 protons, in the methylene group there are 2 protons, hence the torsional motion of ethyl group is responsible for such a great intensity of the corresponding peaks.

Observed in the region 390–430 cm^{-1} changes in the $G(\nu)$ spectra *i.e.* the shift in peak position at 424 cm^{-1} in undeuterated to 419 cm^{-1} in deuterated sample of (*E*)-2-cyanoethyl ester-2-oxime is a result of substitution of H by deuterium in the O−H group.

The intensity of the $G(\nu)$ bands also decreased after deuterization. The IINS peaks with rather great intensity are connected with modes of groups with hydrogen atoms in the (*E*)-2-cyanoethyl ester-2-oxime molecule, although also the other parts of the molecules take part in those vibrations. It is also a case for example for peaks at 358.7 and 424 cm^{-1} where bending (deformational in plane) of the bond between oxime and etoxy (C−CO−) group takes place causing some replacement of H atoms.

A comparison of experimental $G(\nu)$ frequencies with theoretical ones (calculated for the most probable conformations from Table 1) in the frequency region up to 1700 cm^{-1} shows that the best agreement between the experimental result and theoretical one is for conformation 1 of a isolated molecule and for the dimer with O(1)−H(1)···O(2) HB shown in Fig. 5.

One can see a lack of theoretical frequencies in the corresponding spectrum of dimer in regions: *ca.* 450–500, 580–600 and 920–1000 cm^{-1} which one can see when

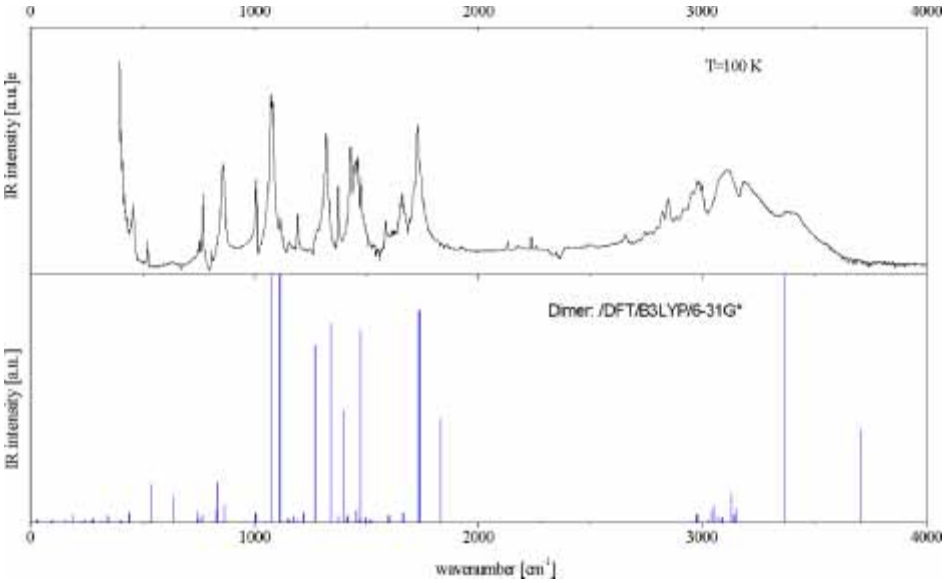

Fig. 6. Comparison of the experimental IR spectra of 2-oxime in KBr taken at 100 K with the calculated ones for dimer by the DFT method with B3LYP/6-31G* basis set.

comparing those regions with the corresponding ones in the experimental IINS experiment. The reason of the event is obvious, namely our theoretical calculations are connected with a dimeric molecule. It is an assumption because in reality there are not only two molecules linked by hydrogen bond but all molecules are bound in such the way.

In the first step of our calculations we obtained the theoretical frequencies also for a single molecule. Generally speaking the theoretical spectrum for dimer is similar to the theoretical spectrum for the single molecule. In spectrum for dimer we can see additional frequencies at *ca.* 20, 50, 190, 300, 420, 560, 660 cm^{-1} which are absent in spectrum for single molecule and present in the INS spectra. We can admit that also dimer molecule model is a simplification of the real situation of molecules in the crystal lattice, which is known from X-ray diffraction and from NPD methods [5].

An inspection of Table 3 reveals that in the energy transfer range from 100 to 1000 cm^{-1} all modes observed by using of optical spectroscopy methods, presented in our previous paper [11] can be also identified by the IINS spectroscopy, with the exception of the γ O−H hydrogen bond modes, which are only observable in the IINS spectra. We mean here the frequencies 335 and 590 cm^{-1}. The other are observed in IINS and in the optical spectroscopy, because not only O−H vibrations appear at certain frequency and the last ones are seen in the optical spectroscopy. If only the corresponding O−H γ vibration had appeared at the frequency it would not have been seen in the optical spectroscopy.

Figure 6 shows a comparison of IR spectra taken at 293 K and calculated frequencies and intensities of modes active in IR spectra for dimer forming O(1)−H(1)···O(2) hydrogen bridge bond. The calculated scaling factor is 0.97 (Fig. 7), what means that

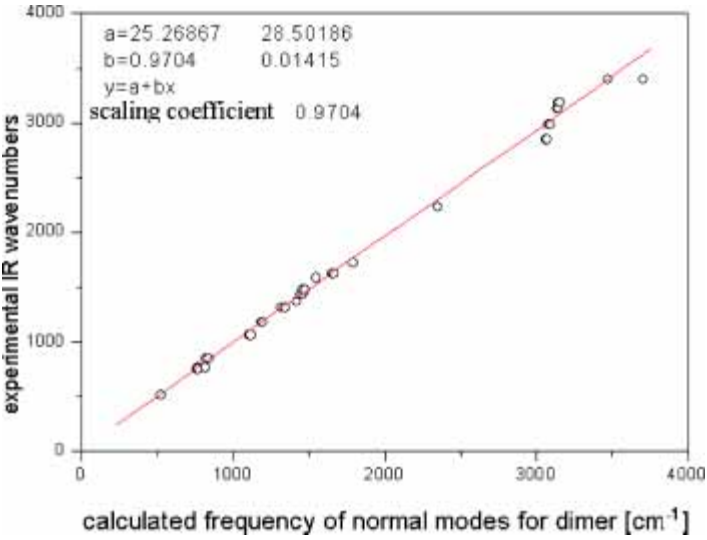

Fig. 7. Scaling procedure between IR frequencies and those obtained from calculations.

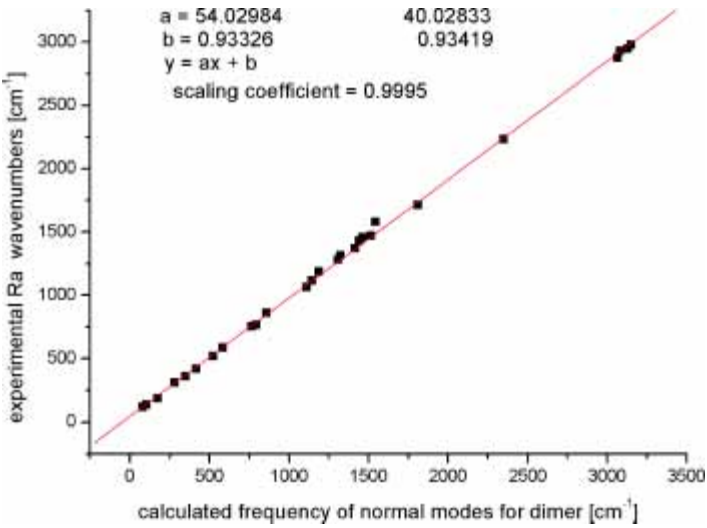

Fig. 8. Scaling procedure between Ra frequencies and those obtained from calculations.

the harmonic approximation seems to be good. The calculated scaling factor has been calculated also for the comparison between experimental Ra frequencies and those calculated (Fig. 8) and it shows also that the harmonic approximation seems to be good as it was a case in Fig. 7.

These results demonstrate the advantage and usefulness of IINS experiments in the study of molecular dynamics in the crystals which contain hydrogen bond networks, as for example in oximes.

It is impossible to reproduce the low frequency bands in the experimental spectrum of 2-oxime taking into account separate molecule. Theoretical spectrum of the 2-oxime dimer linked by OHO hydrogen bonds reproduces the low frequency region quite well, although comparison of the experimental and theoretical spectra suggests as worth taking into account higher polymer and probably also chain and cyclic structures linked by many hydrogen bonds reflected in the low frequency region.

5. Conclusion

Formation of the hydrogen bonded dimer of 2-oxime is reflected in the vibrational spectrum. The ν(OH) stretching vibration band shifts to lower frequencies. In-plane bending δ(O−H) vibration is coupled to other δ vibrations of 2-oxime and formation of the dimer causes shifting of the vibrations with participation of δ(OH) to higher frequencies. The similar situation we have for σ(O−H) and γ(O−H) frequencies. In the low frequency range there arise the bands most characteristic for hydrogen bond bridge (stretching σ and bending λ, γ-bending out of plane) well reproduced in the experimental INS spectrum. For this reason the INS spectroscopy is the best method of investigation of the low frequency range of vibrational spectrum not accessible with other spectroscopic methods for samples with H-atoms.

Acknowledgement

The possibility to present the X-ray results during the conference: 13th International Seminar on Neutron Scattering Investigation in Condensed Matter (8–10 May 2008, Institute of Physics, UAM, Poznań, Poland) is fully acknowledged by the authors.

The QC calculation were performed under the grand at PSCC in Poznań, some of them namely connected with conformations of single molecule were done by means of Baribal computer in Cyfronet (Kraków, Poland).

References

1. G. A. Jeffrey and W. Saenger, *Hydrogen Bonding in Biological Structures*, Springer, Berlin (1991).
2. A. Novak, J. Chim. Phys. **69** (1972) 1615.
3. I. A. J. Dianox and G. Lander, Neutron Data Booklet ILL, Neutron for Science, Grenoble (2002).
4. L. H. Minaczeva, I. W. Raspiertoba, T. Sliwa, and R. D. Lampieka, Koord. Chim. **26** (2000) 235.
5. I. Natkaniec *et al.*, to be published (2011).
6. E. Juszczyńska, M. Massalska-Arodż, I. Natkaniec, *et al.*, Physica B **403**(1) (2008) 109.
7. A. Pawlukojc, W. Starosta, J. Leciejewicz *et al.*, Chem. Phys. Lett. **437**(1–3) (2007) 32.
8. K. Hołderna-Natkaniec, I. Natkaniec, and W. Kasperkowiak, J. Mol. Struct. **790**(1–3) (2006) 94.

9. B. Hudson, J. S. Tse, M. Z. Zgierski, S. F. Parker, D. A. Braden, and C. Middleton, Chem. Phys. **261** (2000) 249.
10. Mercury CSD 2.0, C. F. Macrae, J. A. Bruno, J. A. Chisholm, P. R. Edgington, P. McCabe, E. Pidcock, L. Rodriguez-Monge, R. Taylor, J. van de Streek, and P. A. Wood, J. Appl. Cryst. **41** (2008) 466.
11. M. Rachwalska and Z. H. Urbanek, Z. Phys. Chem. **222** (2008) 1625.
12. D. S. Jackson, J. Chem. Soc. (B) (1969) 785.
13. (a) R. S. Cahn, C. K. Ingold, and V. Prelog, Experientia **12** (1956) 81; (b) R. S. Cahn, C. K. Ingold, and V. Prelog, Angew. Chem. Int. Ed. Eng. **5** (1966) 385; (c) J. Mohurray, Organ. Chemi. (Polish Edn.) (2004) 188–190.
14. A. Pawlukojc, K. Bajdor, J. Cz. Dobrowolski, J. Leciejewicz, and I. Natkaniec, Spectrochim. Acta A **53** (1997) 927.
15. A. Pawlukojc, L. Bobrowicz, and I. Natkaniec, Spectrochim. Acta A **51** (1995) 303–308.
16. A. Pawlukojc, J. Leciejewicz, J. Tomkinson, and S. F. Parker, Spectrochim. Acta A **57** (2001) 2513.
17. M. Conrad and A. Schalze, Chem. Ber. **42** (1909) 735.
18. I. Natkaniec, S. I. Bragin, J. Brańkowski, and J. Mayer, in: Proceedings of the ICANS XII Meeting, Abingdon 1993, RAL. Report 94-025, Vol. I.I (1994), pp. 89–96.
19. V. V. Sikolenko (ed.), User Guide-Neutron Experimental Facilities for Condensed Matter Investigations at FLNP JINR Dubna (1997), pp. 27–29.
20. W. J. Kazimirov and I. Natkaniec, Programme for Calculation of the Resolution Function of NERA-PR and KDSOG-M Inelastic Neutron Scattering Inverse Geometry Spectrometers, Preprint P14-2003-48 JINR, Dubna (2003).
21. A. J. Ramirez-Cuesta, Comp. Phys. Commun. **157** (2004) 226–238.
22. Gaussian 03, Revision D.01, M. J. Frisch, G. W. Trucks, H. B. Schlegel, G. E. Scuseria, M. A. Robb, J. R. Cheeseman, J. A. Montgomery Jr., T. Vreven, K. N. Kudin, J. C. Burant, J. M. Millam, S. S. Iyengar, J. Tomasi, V. Barone, B. Mennucci, M. Cossi, G. Scalmani, N. Rega, G. A. Petersson, H. Nakatsuji, M. Hada, M. Ehara, K. Toyota, R. Fukuda, J. Hasegawa, M. Ishida, T. Nakajima, Y. Honda, O. Kitao, H. Nakai, M. Klene, X. Li, J. E. Knox, H. P. Hratchian, J. B. Cross, V. Bakken, C. Adamo, J. Jaramillo, R. Gomperts, R. E. Stratmann, O. Yazyev, A. J. Austin, R. Cammi, C. Pomelli, J. W. Ochterski, P. Y. Ayala, K. Morokuma, G. A. Voth, P. Salvador, J. J. Dannenberg, V. G. Zakrzewski, S. Dapprich, A. D. Daniels, M. C. Strain, O. Farkas, D. K. Malick, A. D. Rabuck, K. Raghavachari, J. B. Foresman, J. V. Ortiz, Q. Cui, A. G. Baboul, S. Clifford, J. Ciosłowski, B. B. Stefanov, G. Liu, A. Liashenko, P. Piskorz, I. Komaromi, R. L. Martin, D. J. Fox, T. Keith, M. A. Al-Laham, C. Y. Peng, A. Nanayakkara, M. Challacombe, P. M. W. Gill, B. Johnson, W. Chen, M. W. Wong, C. Gonzalez, and J. A. Pople, Gaussian, Inc., Wallingford CT, 2004.
23. J. Kalus, Ann. Phys. **7** (1972) 247.
24. C. F. Macrae, P. R. Edgington, P. McCabe, E. Pidcock, G. P. Shields, R. Taylor, M. Towler, and J. van de Streek, J. Appl. Cryst. **39**(3) (2006) 453.
25. I. J. Bruno, J. C. Cole, P. R. Edgington, M. K. Kessler, C. F. Macrae, P. McCabe, J. Pearson, and R. Taylor, Acta Cryst. B **58** (2002) 389.
26. R. Taylor and C. F. Macrae, Acta Cryst. B **57** (2001) 815; The Cambridge Structural Database, F. H. Allen, Acta Cryst. B **58** (2002) 380.
27. I. J. Bruno, J. C. Cole, P. R. Edgington, M. Kessler, C. F. Macrae, P. McCabe, J. Pearson, and R. Taylor, Acta Cryst. B **58** (2002) 389.
28. P. J. Stevens, F. J. Devlin, C. F. Chabałowski, and M. J. Frisch, J. Chem. Phys. **98** (1994) 11623.
29. R. Krishnan, J. S. Binkley, R. Seeger, and J. A. Pople, J. Chem. Phys. **72** (1980) 650.
30. R. Ditchfield, W. J. Hehre, and J. A. Pople, J. Chem. Phys. **54** (1971) 724.
31. C. J. Cramer, *Essentials of Computational Chemistry. Theories and Models*, John Wiley and Sons Ltd, Buffins Lane, Chichester, West Sussex, England (2002).
32. W. Koch and M. C. Holthausen, *A Chemist's Guide toDensity Functional Theory*, 2nd Edn., Wiley-VCH, Weinheim (2001).

33. T. R. Fukuto, R. Mecalf, R. L. Jones, and R. O. Myers, J. Agric. Food Chem. **17**(5) (1969) 923.
34. P. Kovacic, Curr. Med. Chem. **10**(24) (2003) 2705.
35. H. Dai, H.-B. Yu, J.-B. Liu, Y.-Q. Li, X. Q. Zhang, Z.-F. Qin, T.-T. Wang, and J.-X. Fang, ARKIVOC **VI** (2009) 126.
36. E. Abele, R. Abele, and E. Lukevics, Chem. Heterocycl. Compd. **39**(7) (2003) 825.

Supplement

Some details connected with neutron scattering experiments

The NERA spectrometer allows the recording of the IINS and NPD spectra from 0.5 to 7 Å of incident neutron wavelengths. The 16 IINS spectra are recorded at scattering angles from 20 up to 160°, with an interval of 10°. Simultaneously, several detectors could record the NPD spectra at two sectors of the scattering angles: 120–150° and 30–60°, which practically allows the measuring of lattice spacing in the range of 0.1–1 nm. The incident neutron wavelength of the NPD spectra is determined by measuring the neutron time-of-flight along the IBR-2 moderator to the NPD detector distance of 110.45 m. This allows determining the lattice spacing in the range of 0.2–0.5 nm within the resolution of 0.2–0.5%, using the real neutron pulse width (0.2–0.3 ms) of the IBR-2. In the case of inelastic scattering, the energy of scattered neutrons is selected by the cooled beryllium filters and pyrolytic graphite neutron wave length analyzers, placed before the detectors. The elastic line of the NERA spectrometer is fixed at a neutron wave length of 4.25 Å, which corresponds to 4.53 meV of the final energy of scattered neutrons. The full width at half maximum (FWHM) of the elastic line is 0.6 meV. The incident neutron energies for the IINS are determined by measuring the neutron time-of-flight along the IBR-2 moderator to the sample distance of 109.05 m. The incident neutrons are transported from the moderator by the Ni-coated mirrored guide tube of rectangular shape (dimensions: 60 mm wide, 160 mm high and 100 m long). The resolution power of the NERA-PR spectrometer increased continuously from 2 to 4% when energy transfer increased up to 4000 cm^{-1} (500 meV) [20].

INS in inverted geometry involve only neutrons with energy loss. In the technique of inverted geometry of INS we count only cold neutrons after their “reaction” with the sample. They were warm at the very beginning of the experiment coming to the sample with various velocities (energies) and they got cold because their energy was obtained by vibrations in the sample. Only those are detected which pass the Beryllium filter. The energies of neutrons coming to the sample and energy of neutron after scattering, after passing the Beryllium filter could be easy estimated. Hence we obtain energy transfer of neutrons for vibrations in the sample. The results received for the investigated sample are presented in Fig. 2. The schematic presentation of the inverted geometry time of flight spectrometer is shown in the Fig. 9 (in *Supplement*).

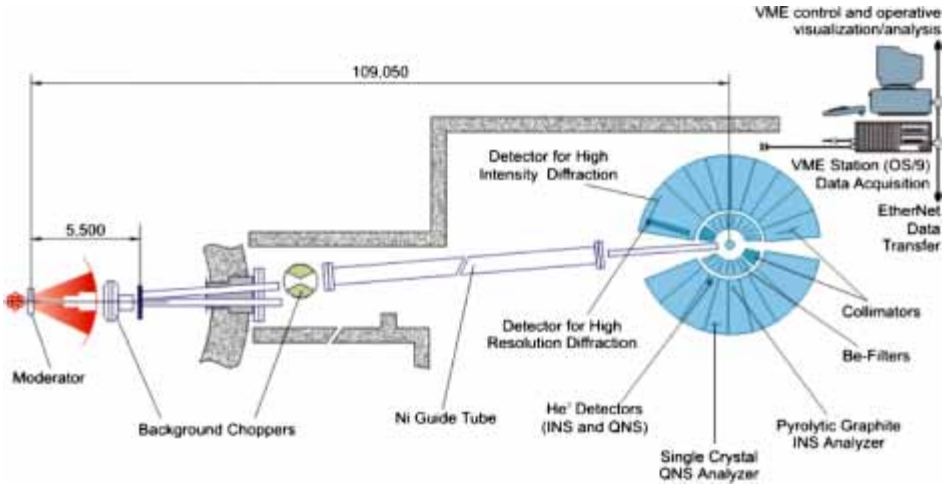

Fig. 9. Inverted geometry time of flight spectrometer NERA at the IBR-2 high flux pulsed reactor in Dubna [18].